Carnegie Observatories Astrophysics Series, Vol. 3:
Clusters of Galaxies: Probes of Cosmological Structure and Galaxy Evolution, 2004
ed. J. S. Mulchaey, A. Dressler, and A. Oemler (Pasadena; Carnegie Observatories:
http://www.ociw.edu/ociw/symposia/series/symposium3/proceedings.html)

The Density-Morphology-Star Formation Rate Relationship for SDSS Galaxies

C. J. MILLER
Carnegie Mellon University

Abstract

We present an analysis of the effect of environment on the star–formation rate (SFR) and active galactic nuclei (AGN) activity of galaxies within the early data release of the Sloan Digital Sky Survey (SDSS). We have used the Hα emission line to derive the star–formation rate (SFR) for each galaxy within a volume-limited sample of galaxies with $0.05 \leq z \leq 0.095$ and $M(r^*) \leq -20.45$. We find that the median SFR of galaxies is strongly correlated with the local (projected) galaxy density and thus we present here the *density–SFR relation* that is analogous to the density–morphology relation. We confirm that the fraction of star-forming galaxies dramatically decreases in dense regions, while the fraction of passively classified galaxies increases. After separating the star-forming population of emission-line galaxies from the AGNs, we show that the fraction of AGNs is constant over all densities. We use a cluster sample to relate our pseudo-3D galaxy densities to virial radii, and show that the median SFR of galaxies begins to decrease at ~ 2 virial radii (or projected surface density of one galaxy per square megaparsec). We show that the tail of the SFR distribution is populated by late-type spirals, and that the median SFR of spirals decreases as a function of density. Finally, we show that the fraction of spiral galaxies with an AGN is similar to the entire galaxy population and is independent of local density.

1.1 Introduction

A fundamental goal of observational cosmology is to determine the spatial distribution of galaxies as a function of galaxy properties, *e.g.*, luminosity, morphology, star formation rate *etc.*, as such observations place constraints on models of galaxy formation and evolution. In recent years, there has been an explosion in such work due to improvements in the theoretical modeling of galaxy evolutionary processes (*e.g.*, Kauffmann et al. 1999; Benson et al. 2002) and the availability of large amounts of high quality survey data, *e.g.*, Sloan Digital Sky Survey (SDSS; York et al. 2000), 2dF Galaxy Redshift Survey (Colless et al. 2001).

Observational work of recent years has demonstrated that there has been a significant decline in the global star–formation rate of the Universe with time (Lilly et al. 1996; Madau et al. 1996). In models of hierarchical structure formation, the cosmic star formation history is driven partly by internal processes (i.e., gas consumption) and partly by environmental effects (Kauffmann et al. 1993; Cole et al. 2000; Sommerville and Primack 1999). It is believed that these processes affect the amount of gas in galaxies which is the basic fuel for the star formation activity. For instance, galaxies in groups and clusters which are not located at the center of their potential are assumed to have no hot gas reservoir with which to refuel the cold gas available for star formation. As a consequence, the star formation rates of galaxies in dense environments quickly decline (Diaferio 2001; Baugh et al. 1996; Balogh et al. 2000). In addition, galaxies in dense environments may experience a variety of other effects which are not included in these models, such as ram pressure stripping of the cold gas due to interaction with the intracluster medium (Gunn and Gott 1972), galaxy harassment from high velocity encounters with other galaxies (Moore et al. 1999) tidal disruption (Byrd and Valtonen 1990) or galaxy evolution via mergers and close encounters in infalling poor groups (Zabludoff and Mulchaey 1998). The interpretation of the global decline in star formation, then, requires us to distinguish between internal effects and the effects of the local or large scale environment on star formation.

Likewise, there have been similar observational efforts to study the local environments of active galactic nuclei (AGN). Early works by Dressler et al. (1985) and Huchra and Burg (1992) found that AGN were less likely to be found in clusters than in the field. However, more recent analyses (e.g. Ho et al. 1997; Carter et al. 2001, Miller et al. 2003) are finding AGNs in all environments. Under the hypothesis that an active nucleus indicates the presence of a black hole, which in turn can be tied to the formation of the galaxy, than the distribution of galaxies with AGNs plays an important role in understanding galaxy evolution. For example, an AGN could be fueled by the same cold gas in the disk component of galaxies that is driving the star–formation rate (SFR) of those galaxies. In this case, the existence of an AGN might diminish in dense regions, analogous to the SFR-density relation (see Lewis et al. 2002; Gomez et al. 2003, Carter et al. 2001, this work). Alternatively, several authors have proposed that galaxy–galaxy collisions fuel the AGN activity by driving gas into the cores of galaxies and thus onto the black hole (Gunn 1979; Shlosman 1990). A third possible empirical model proposed by Kormendy & Gebhardt (2001) suggests that supermassive black holes are solely a bulge phenomena and were formed at the same time as the bulge component of galaxies at an much earlier epoch in the Universe. In this model, the distribution of AGNs would then trace the distribution of bulges, under the assumption that AGNs are powered by supermassive black holes (Lynden–Bell 1964).

As a first step in addressing these issues, we use the Early Data Release (EDR; Stoughton et al. 2002) of the Sloan Digital Sky Survey to further understand the relation between environment, the star–formation rate of galaxies, and AGN activity. The EDR is an excellent database for such a study because it provides a large, homogeneous sample of galaxies, with a medium resolution, flux–calibrated spectrum and 5 passband photometry, over a wide range of environments. Such data allows for the computation of the Hα, and OII, equivalent widths (EW) and star-formation rates (SDR) for all galaxies in a self–consistent way. Our work expands upon earlier cluster studies in four key ways. First, we probe the rarefied field and poor group regimes, which include the most common galactic environments in the Universe. Second, we focus on the low redshift universe ($z \leq 0.1$), which provides a zero–point for the high redshift studies. Third, we are able to follow the activity (either through star–formation or AGN of galaxies continuously, and with excellent galaxy statistics, from the cores of rich clusters and poor groups into the rarefied field. Finally, we can accurately quantify the local galaxy density in a uniform manner that is not subject to statistical background correction.

1.2 Results

1.2.1 Star-formation versus Density

The star formation rates of galaxies can be indirectly determined in various ways, as reviewed by Kennicutt (1998). The most successful methods rely on correlations of the star formation rate with measurements of the far-infrared luminosity (which arises from dust heated by star formation), the radio luminosity (which results from synchrotron emission associated with supernovae) and indicators that are sensitive to the ionizing flux from massive stars. The last category includes measurements of the ultraviolet continuum and the fluxes of nebular emission lines. Each of these techniques is subject to different biases and calibration uncertainties, but does give consistent estimates for "normal" galaxies when these effects are accounted for. In this proceeding, we focus on SFRs estimated from the Hα line. Dust extinction is the largest source of uncertainty, as both the effective optical depth and dust geometry must be considered.

We investigate the SFR of galaxies as a function of their local galaxy density. We can parameterize the local environment of each galaxy using the projected density of galaxies in a manner similar to that employed by Dressler (1980). This involves calculating the projected distance to the 10^{th} nearest spectroscopically–observed neighbor, and then converting that into a surface density ($h_{75}^{-1} Mpc^{-2}$). Our magnitude limit is $M(r^*) = -20.45$ ($h = 0.75$), which is close to the limit used by Dressler ($M(V) = -20.4$, $h = 0.5$). Our methodology does differ from that used by Dressler (1980) in that we use a circular search aperture (instead of a rectangle) and spectroscopically eliminate foreground and background galaxies so no further background correction is necessary. Thus our tenth nearest neighbor will be farther away than obtained via Dressler's definition. Therefore, our effective "smoothing" scale is larger, and we may not be as sensitive as Dressler (1980) to the densest environments, *i.e.,* cluster cores.

When calculating the local density, edge effects are particularly important because the EDR geometry is long strips of data that, at the median redshift of our sample, subtend $14.8\,h_{75}^{-1}$ Mpc on the sky. To account for this, we remove any galaxy in which less than 75% of the circular area including the 10^{th} nearest neighbor lies within the EDR boundary. We do not make an area correction to our density estimates because we do not know if the 10^{th} nearest neighbor we have observed is, in fact, the true 10^{th} nearest neighbor. If it is, then correcting the density estimates for the area outside the survey boundary would bias the density estimates of those galaxies. Instead, we accept the fact that $\sim 25\%$ of galaxies near the edge of the survey have an incorrect local density measurement but that they are not preferentially biased. We have checked the effect of changing our tolerance to accepting galaxies near the edge of the survey, from rejecting all galaxies where the 10^{th} nearest neighbor is closer than any survey boundary, to including all galaxies regardless of edge effects, and find our results are robust.

In Figure 1.1 (Left), we present the Hα star-formation rate distribution as quantified by the median, the 25^{th}, and the 75^{th} percentiles, versus local density as defined above. The star-formation rates have been normalized by the z-band luminosity of each galaxy. We see an overall shift of these distributions to lower values in high density regions. We note that this plot shows how the distribution of galaxy star-formation rates changes as a function of density (and not necessarily how the star-formations themselves change).

We now turn our attention to virialized systems like clusters and groups of galaxies, and

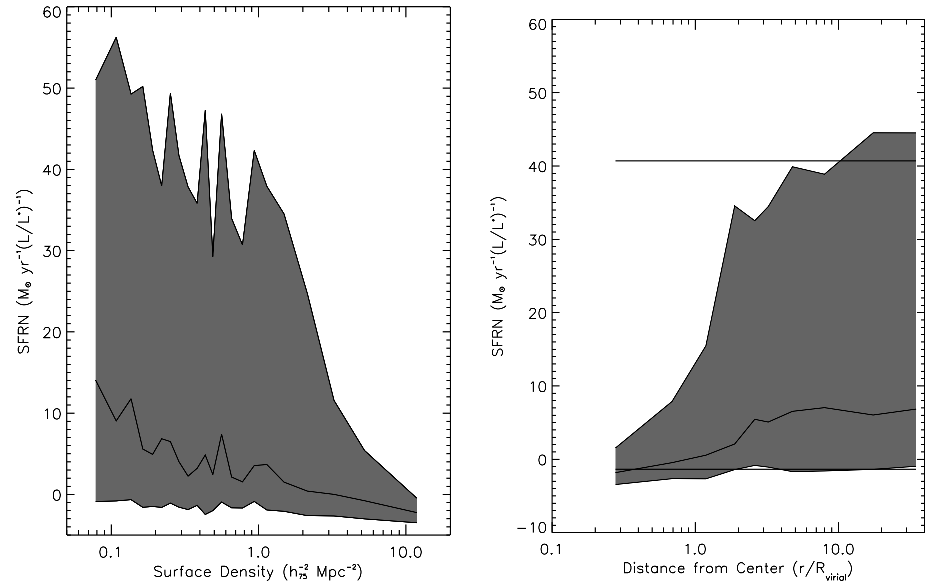

Fig. 1.1. (**Left**): The Hα star-formation rate, normalized by the z-band galaxy luminosity, as a function of density. The upper edge of the grey band corresponds to the 75^{th} percentile of star-formation rate distribution in each bin, while the lower edge corresponds to the 25^th percentile. The median is the solid line. Note the sharp decrease for densities greater than one galaxy per square Mpc. (**Right**): The Hα star-formation rate, normalized by the z-band galaxy luminosity, as a function of distance to the nearest cluster (normalized by the cluster virial radius).

investigate the SFR of galaxies as a function of clustercentric radius. We test whether the features observed in the density–SFR relation, (*e.g.,* the break or characteristic density at $\sim 1\,\mathrm{h}_{75}^{-2}\,\mathrm{Mpc}^{-2}$) are also present in the radius–SFR relation around known virialized systems. For details of how we objectively select clusters please see Nichol et al. 2004 (this Proceeding).

In Figure 1.1 (Right), we present the observed distribution of Hα star-formation rates quantified by the median, 25^{th}, and 75^{th} percentiles versus (projected) clustercentric radius for 17 groups and clusters of galaxies detected in the EDR data. Again, the star-formations have been normalized by the z-band galaxy luminosity. To accommodate the wide range of masses spanned by our cluster sample, we have re–scaled all radial distances by the virial radius (R_v) of each cluster. R_v is computed from the line–of–sight velocity dispersion, in units of km s^{-1}, using the formula $R_v \simeq 0.002\sigma_r h_{100}^{-1}$ Mpc from (Girardi et al. 1998). Notice that the star-formation drops off steeply as a function of radius at about ~ 2 virial radii. This radius corresponds to about one galaxy per square megaparsec as seen in Figure 1.1 (Left).

1.2.2 AGN Fraction versus Density

To classify AGNs, we use the traditional log(OIII/Hβ) versus log(NII/Hα) flux-ratio diagnostic diagrams as discussed by Baldwin, Philips & Terlevich (1981), Villieux & Osterbrock (1987) and Kewley et al. (2001). The flux of these emission lines are determined using the fitted heights and sigmas of the lines as measured by the SDSS data analysis pipeline. We restrict our analysis to lines with a measured flux over flux error of > 2, *i.e.*, $> 2\sigma$ detections.

We note here that it is not necessary to possess significant detections of all four of these lines (NII, OIII, Hα and Hβ) to unambiguously detect an AGN in a galaxy; although one does need all four lines to unambiguously classify star-forming galaxies. For example, if a galaxy has NII and Hα lines detected at $> 2\sigma$ confidence, but no significant detection of OIII or Hβ, we can still classify it as an AGN if log(NII/Hα)> -0.2. In fact, the majority of AGNs in the SDSS EDR are classified using only the NII and Hα lines, which has two important advantages compared to the 4–line method. First, the classification is unambiguous, since we have chosen line ratios high enough to exclude nearly all star–forming galaxies in Figure 1. Second, NII and Hα are close together in wavelength so we have no concerns about the amount of internal dust extinction when classifying these galaxies.

In Figure 1.2, we plot the fraction of galaxies in each of our classifications (star–forming, passive, AGN) as a function of the projected local galaxy density, which is identical to that described in the previous section. Figure 1.2 shows the expected decrease in the fraction of star–forming galaxies in dense regions and the increase in the fraction of passive galaxies in dense environments. These relations are analogous to SFR–density and morphology–density relations of Gomez et al. (2003) and Dressler et al. (1997) respectively. We find that the AGN fraction is constant over the two orders of magnitude in local galaxy density probed by this work, *i.e.*, spanning a density range that includes the cores of rich clusters to the rarefied field population. The small decrease in the AGN fraction in the densest regions is not statistically significant; a line with zero slope is a good fit to the fraction versus density. The fraction of galaxies which exhibit AGN activity is at is $\sim 20\%$.

In addition, we have performed chi-square tests on the fraction distributions in Figure 1.2 (Left). In this analysis, we measured the chi-square test statistic using the mean of the fraction per galaxy type as the null hypothesis. This test then tells us whether we can rule out a constant fraction (defined by the mean) as a function of density for each galaxy type. For AGN, we can only rule out a constant AGN fraction at the 46% level (i.e., a constant AGN fraction cannot be ruled out for this data). On the other hand, we can rule out a constant star-forming fraction at the $>99.9999\%$ level, and a constant fraction of passive galaxies is ruled out at the 99.999% level. We have looked at this statistic using only 2–line or 4–line AGNs as defined above and also find that the a mean constant fraction cannot be ruled out for the either of these subsets of AGNs. We can restate this result in that the dip in the innermost bin of the AGN fraction seen in Figure 1.2 (Left) is not significant. We note that there is a significant number of emission-line galaxies which could not be classified in this bin. These objects are either star-forming or AGN, and when we model the distribution of AGNs in the unidentified sample, we conclude that probably 40% of galaxies in our magnitude and volume-limited sample contain an AGN. The fraction of AGNs versus density after we apply this modeling is showing in Figure 1.2 (Right).

1.2.3 Morphology

We use the (inverse) concentration index C_{in} of SDSS galaxies as a proxy for galaxy morphologies (Shimasaku et al. 2001). This parameter can be used as an objective morphological classification under certain, well-defined circumstances. However, it is hard to interpret and to compare the concentration index directly with the visual morphologies. Although concentration will be sensitive to non-morphological features like the presence of

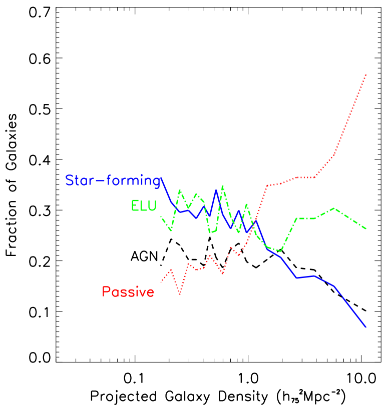

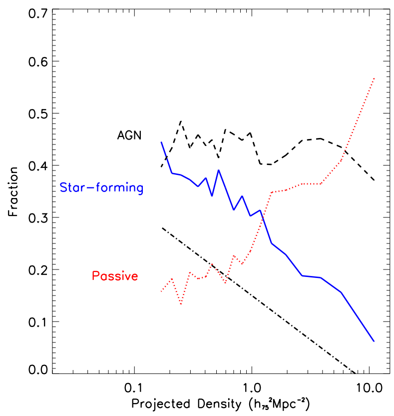

Fig. 1.2. (**Left**) The fraction of galaxies as a function of the different spectral classifications, in our pseudo volume-limited sample, as a function density. We see an increase in the fraction of passive galaxies with density, and a decrease in the fraction of star–forming galaxies with density. This is the SFR-density (Gomez et al. 2003) and morphology-density (Dressler 1980; Dressler et al. 1997) relations. The ELUs are galaxies with at least one emission-line that could not be classified (due to lack of enough lines). (**Right**) We model the AGN/star–forming distribution of ELU galaxies. This model (the dot-dash line) requires that the overall fraction of star–forming galaxies in dense regions remains small. The passive fraction remains unaltered. *The fraction of galaxies possessing an AGN is statistically–consistent with a constant over all local galaxy densities probed here* The fraction of AGNs in this sample is $\sim 20-40\%$, depending on whether the ELUs are modeled.

nuclear star-formation, there appears to be a reasonable relation between *Cin* and the Hubble morphological classifications as shown in Figure 10 of Shimasaku et al. (2001). For the analysis in this paper, we have chosen a threshold of $C_{in} > 0.4$ to define late–type galaxies, instead of $C_{in} > 0.33$ as proposed by Shimasaku et al. (2001), as this provides a cleaner, but more incomplete, sample of such galaxies. We estimate from Figure 10 of Shimasaku et al. (2001) that this higher threshold ensures less than 5% contamination from early–type galaxies in the late–type sample. Thus, we can create a relatively pure but incomplete sample of late-type galaxies using the concentration index.

To study early type galaxies, we avoid the use of the concentration index, as those galaxies with $C_{in} < 0.33$ are highly contaminated with S0 type galaxies. Instead, we use those galaxies which are members of clusters, under the hypothesis that the density-morphology relation is particularly well-known and established inside galaxy clusters. Simply put, we assume that the cores of galaxy clusters are comprise of old elliptical galaxies. We discuss this in more detail below.

1.2.4 Star-formation-Morphology-Density

We find that the tail of the star-formation rate distribution is dominated by late–type (spiral) galaxies regardless of local density, *i.e.,* $> 75\%$ of all galaxies with Hα EW > 5Å are consistent with being late–type galaxies. In Figure 1.3 we plot the star-formation rate distribution as a function of density for galaxies with low and high concentration indices.

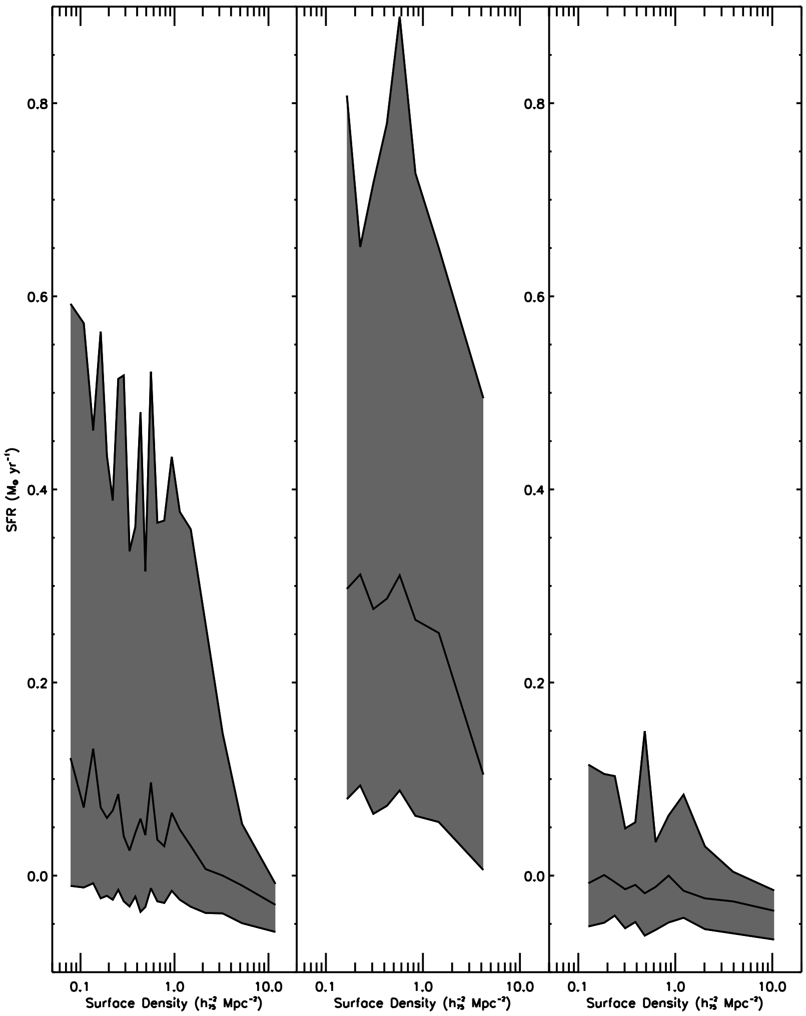

Fig. 1.3. (Left panel) The same as shown in Figure 1.1, except that the star-formation rates are not normalized by the galaxy luminosities. (Middle panel) The density–SFR for late-type galaxies (*i.e.*, with $C_{in} > 0.4$ as discussed in the text). As in other plots, the top of the shaded area is the 75^{th} percentile of the distribution, while the bottom of the shaded region is the 25^{th} percentile of the distribution. The median is shown as a black line near the middle of the shaded region. (Right Panel) The density–SFR for galaxies with $C_{in} \leq 0.4$).

Again, those with high $C_{in} > 0.4$ are most likely a clean sample of late-type spiral galaxies, while those with low $C_{in} < 0.4$ are undoubtedly a mixture of old ellipticals, S0s, etc. We see that the median star-formation of late-type spirals decreases with increasing density. Unfortunately, we have too few galaxies to probe the highest density regions.

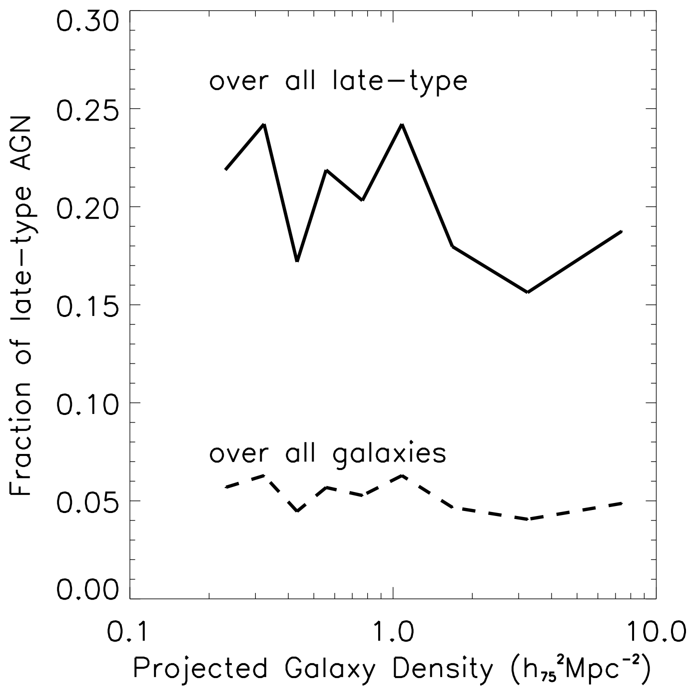

Fig. 1.4. The solid-line shows the fraction of just late–type (spiral) galaxies that have an AGN. While the dashed-line shows the fraction of all galaxies that are both late–type and have an AGN. This figures shows that late–type galaxies have the same AGN fraction as all galaxies, and there is again no dependence on density. The late-types are identified using the Concentration Index (as described in the text). This classification scheme creates a pure, but incomplete sample of late-type galaxies. Thus, the dashed-line is difficult to interpret due to this incompleteness.

1.2.5 AGN Fraction, Morphology, Density

In this section, we study the fraction of AGNs in galaxies as a function of the morphology of the host galaxy. First, we utilize the inverse concentration index (C_{in}) in the SDSS r band, as defined above. In Figure 1.4, we present the AGN fraction for galaxies with $C_{in} \geq 0.4$ (late–type galaxies) as a function of local galaxy density. We observe no trend with density for just the late–type (spiral) galaxies and the fraction of all late–type galaxies with an AGN is $\sim 20\%$, similar to the entire galaxy population (see Figure 1.2 (Left)).

To study the fraction of early–type galaxies with an AGN, we can not use $C_{in} < 0.4$ as this sample is severely contaminated by late–type galaxies (see Gomez et al. 2003; Shimasaku et al. 2001; Strateva et al. 2001). As an alternative, we can study the subset of galaxies that reside in known clusters of galaxies, as these galaxies will be predominately early–type (ellipticals and S0's) galaxies. To achieve this goal, we use the C4 cluster catalog which was described in Gomez et al. (2003) and Nichol (2004). In this paper, we use a sample of 23 C4 clusters in the EDR area that have a mean redshift between $0.053 \leq z \leq 0.092$. We then select 967 galaxies from our original sample that lie within a projected distance of 2 virial radii from one of these clusters, and within $|z_{galaxy} - z_{cluster}| \leq 4\sigma_v$, where σ_v is the velocity dispersion of the clusters. As expected, we find that the fraction of star–forming galaxies is lower for these cluster galaxies than for our full sample. As seen in Gomez et al. (2003), the fraction of star–forming galaxies becomes significantly lower in the inner (projected) 500kpc of these 23 clusters. Likewise, the fraction of passive galaxies (no detected emission lines) is higher in clusters than for the full sample, and continues to increase towards the inner (projected) 500kpc of our clusters. However, we again observe that the fraction of galaxies with an AGN remains nearly the same in our 23 clusters as for our full sample, and we only witness a small decrease (which is statistically insignificant) in the fraction of AGNs within the inner (projected) 500kpc of our clusters.

1.3 Conclusions

We have investigated the effects of the local galaxy environment on the star–formation of galaxies and the AGN fraction of galaxies. We have used the Early Data Release of the Sloan Digital Sky Survey and restricted our analysis to a volume–limited sample of galaxies brighter than $M(r^*) \leq -20.45$ (k–corrected, for $H_0 = 75\,\mathrm{km\,s^{-1}\,Mpc^{-1}}$) over the redshift range $0.05 \leq z \leq 0.095$. For all galaxies, we have calculated the star–formation using the Hα relation of Kennicutt (1998) as well as the normalized star–formation rates (SFRN; SFR per unit luminosity) from the SDSS data. We have used line-diagnostic diagrams to classify AGNs. We have quantified the local galaxy environment using the projected distance to the 10^{th} nearest neighbor brighter than $M^{\star}+1$ as well as by measuring the clustercentric distance of galaxies from the cores of known clusters and groups of galaxies.

This work expands upon previous studies of SFR of galaxies and AGN fractions as a function of environment in four ways: *i)* We extend such studies into the group and poor cluster regime; *ii)* We focus on the low redshift universe; *iii)* We have traced the SFR activity of galaxies well beyond the cores of the clusters and groups into the field population. Likewise, we have measured the AGN fraction over this same range of density for a statistically complete sample; and finally *iv)* We are able to accurately quantify the local galaxy density in a uniform manner that is not subject to statistical background correction.

The distributions of star-formation rates, as quantified by the median and 25^{th} and 75^{th} percentiles, changes as a function of local galaxy density as measured using the distance to the 10^{th} nearest neighbor. We witness similar relations in the normalized star-formation rates of galaxies (see Gomez et al. 2003). This effect is characterized in three ways. First, there is shift in the overall distributions to lower values with increasing galaxy density. Secondly, the skewness of the distributions decreases with increasing local galaxy density, *i.e.,* the tail of strongly star–forming galaxies (Hα EW > 5Å), as quantified by the 75^{th} percentile of the distribution, is noticeably decreased in high density regions. Finally, we see a "break" (or characteristic scale) in the correlation between SFR and SFRN and density at a local galaxy density of $\simeq 1\,h_{75}^{-2}\,\mathrm{Mpc}^{-2}$ (considering galaxies brighter than M^*). The density corresponds to ~ 2 virial radii outside clusters.

The overall fraction of galaxies with an AGN is $\sim 20\%$ (with an unambiguous classification), but maybe as high as 40% if we have correctly modeled the unclassified emission line galaxies in our sample. This confirms the earlier observations by Ho et al. (1997); Unlike the SFR-density relation, or star-forming fraction-density relation, the AGN fraction is independent of the local density, as well as morphological type of the host galaxy, there appears to be no overall relationship between the star–formation activity in the disk component of galaxies and the presence of an AGN. A plausible interpretation of this result is that the AGN phenomenon is related to the bulge component of galaxies, which is consistent with the hypothesis that a supermassive black hole resides in the bulge of all galaxies (see Kormendy & Gebhardt 2001);

References

Baldwin, J. A., Phillips, M. M., & Terlevich, R. 1981, PASP, 93, 5
Balogh, M. L., Navarro, J. F., & Morris, S. L. 2000, ApJ, 540, 113
Baugh, C. M., Cole, S., & Frenk, C. S. 1996, MNRAS, 283, 1361
Benson, A. J., Frenk, C. S., & Sharples, R. M. 2002, ApJ, 574, 104
Byrd, G. & Valtonen, M. 1990, ApJ, 350, 89
Carter, B. J., Fabricant, D. G., Geller, M. J., Kurtz, M. J., & McLean, B. 2001, ApJ, 559, 606
Colless, M. et al. 2001, MNRAS, 328, 1039
Diaferio, A., Kauffmann, G., Balogh, M. L., White, S. D. M., Schade, D., & Ellingson, E. 2001, MNRAS, 323, 999
Dressler, A. 1980, ApJ, 236, 351
Dressler, A., Thompson, I. B., & Shectman, S. A. 1985, ApJ, 288, 481
Dressler, A. et al. 1997, ApJ, 490, 577
Cole, S., Lacey, C. G., Baugh, C. M., & Frenk, C. S. 2000, MNRAS, 319, 168
Girardi, M., Giuricin, G., Mardirossian, F., Mezzetti, M., & Boschin, W. 1998, ApJ, 505, 74
Gómez, P. L. et al. 2003, ApJ, 584, 210
Gunn, J. E. & Gott, J. R. I. 1972, ApJ, 176, 1
Gunn, J. E. 1979, Active Galactic Nuclei, Cambridge University Press, 1979, p. 213-225.
Ho, L. C., Filippenko, A. V., & Sargent, W. L. W. 1997, ApJ, 487, 568
Huchra, J. & Burg, R. 1992, ApJ, 393, 90
Kauffmann, G., White, S. D. M., & Guiderdoni, B. 1993, MNRAS, 264, 201
Kauffmann, G., Colberg, J. M., Diaferio, A., & White, S. D. M. 1999, MNRAS, 303, 188
Kennicutt, R. C., J. 1998, ARA&A, 36, 189
Kewley, L. J., Dopita, M. A., Sutherland, R. S., Heisler, C. A., & Trevena, J. 2001, ApJ, 556, 121
Kormendy, J. & Gebhardt, K. 2001, AIP Conf. Proc. 586: 20th Texas Symposium on relativistic astrophysics, 363
Lewis, I. et al. 2002, MNRAS, 334, 673
Lilly, S. J., Le Fevre, O., Hammer, F., & Crampton, D. 1996, ApJL, 460, L1
Lynden-Bell, D. 1964, ApJ, 139, 1195
Madau, P., Ferguson, H. C., Dickinson, M. E., Giavalisco, M., Steidel, C., & Fruchter, A. 1996, MNRAS, 283, 1388
Miller, C.J., Nichol, R.C., Gomez, P.L., Hopkins, A.M., Bernardi, M. 2003, ApJ, 597, 142
Moore, B., Lake, G., Quinn, T., & Stadel, J. 1999, MNRAS, 304, 465
Nichol, R. C. 2004, Carnegie Observatories Astrophysics Series, Vol. 3: Clusters of Galaxies: Probes of Cosmological Structure and Galaxy Evolution, ed. J. S. Mulchaey, A. Dressler, & A. Oemler (Cambridge: Cambridge Univ. Press), in press
Shimasaku, K., Fukugita, M., Doi, M., Hamabe, M., Ichikawa, T., Okamura, S., Sekiguchi, M., Yasuda, N., Brinkmann, J., Csabai, I. ., Ichikawa, S., Ivezić, Z., Kunszt, P. Z., Schneider, D. P., Szokoly, G. P., Watanabe, M., & York, D. G. 2001, AJ, 122, 1238
Shlosman, I., Begelman, M. C., & Frank, J. 1990, Nature, 345, 679
Somerville, R. S. & Primack, J. R. 1999, MNRAS, 310, 1087
Stoughton, C. et al. 2002, AJ, 123, 485
Strateva, I. et al. 2001, AJ, 122, 1861
Veilleux, S. & Osterbrock, D. E. 1987, ApJS, 63, 295
York, D. G., Adelman, J., Anderson, J. E., Anderson, S. F., Annis, J., Bahcall, N. A., Bakken, J. A., Barkhouser, R., & the Sloan collaboration. 2000, AJ, 120, 1579
Zabludoff, A. I. & Mulchaey, J. S. 1998, ApJ, 496, 39